International Journal on Semantic Web and Information Systems
Volume 21 • Issue 1 • January-December 2025

Semantic Web-Enhanced Reinforcement Learning Model for Urban Planning Optimization

Yimeng Liang
Northeast Forestry University, China

Jun Zhang
https://orcid.org/0000-0002-4836-7958
Northeast Forestry University, China

ABSTRACT

As urbanization accelerates, urban planning is essential for enhancing quality of life and sustainability. Current methods struggle with complex spatiotemporal data, limiting real-time feature capture and strategy adjustments. To address this, we propose the Semantic Web-Enhanced Reinforcement Learning-based Urban Planning Optimization Model (SWRL-UPOM). Integrating Semantic Web technologies with Spatio-Temporal Adaptive Multimodal Graph Convolutional Network (STAMFGCN) and Spatio-Temporal Gated Hierarchical Attention LSTM (STGHALSTM), SWRL-UPOM uses reinforcement learning to optimize strategies dynamically. STAMFGCN extracts complex inter-regional relationships from multimodal data, while STGHALSTM models and predicts spatiotemporal pollution evolution. Leveraging Semantic Web for structured data and reasoning, the RL framework iteratively updates strategies based on predicted pollution trends. Experiments show SWRL-UPOM outperforms traditional methods in pollution prediction, strategy optimization, and adaptability to dynamic changes.

KEYWORDS

Urban Planning, Semantic Web Technologies, Reinforcement Learning, Graph Convolutional Network, Long Short-Term Memory Network, Pollution Prediction

INTRODUCTION

With the continuous acceleration of global urbanization, the high-density aggregation of urban populations and industrial activities has led to increasingly complex and diversified issues in resource allocation, traffic organization, cultural activity planning, and environmental governance (Alem & Kumar, 2022; Puchol-Salort et al., 2021). How to reasonably plan urban regional layouts to meet the dual needs of urban operational efficiency and social activity demands, while effectively reducing environmental pollution and resource consumption, has become a critical challenge that urgently needs to be addressed. Traditional urban planning heavily relies on empirical judgment or methods based on simple statistical models. For example, traffic flow evaluations are often calculated using averaged data from fixed time periods, making it difficult to adapt to dynamic peak-time variations and resulting in delayed planning decisions (Laurini, 2018; Liu & Ye, 2023; Sharma et al. 2023). At present, with rapid advancements in data acquisition and computational technologies, research paths

DOI: 10.4018/IJSWIS.371755

that utilize deep learning and artificial intelligence (AI) methods to model complex spatiotemporal data to support urban planning decisions are attracting increasing attention (Dowlatshahi et al., 2021; Gokasar et al., 2023; Khalil et al., 2021; Wang et al., 2022).

Current studies have made initial progress in leveraging big data and AI for urban planning analysis, as represented in Figure 1. For instance, some studies attempted to use geographic information system data (Yu et al., 2021), remote sensing images (Bai et al., 2022), traffic flow data, and pollution indicators for correlation analysis (Orieno et al., 2024), aiming to uncover potential spatial patterns and temporal features to help formulate more targeted planning strategies. However, these methods often have several shortcomings. First, many studies remain focused on using statistical models or traditional machine learning algorithms, which have limited data feature extraction and modeling capacity, making it challenging to fully capture deep structures and spatiotemporal dynamics in high-dimensional heterogeneous data (Zheng et al., 2024). Second, some deep learning-based studies focus solely on single data source predictions, lacking robust capabilities for integrating and adaptively mining multimodal data in the spatiotemporal dimension (Wang et al., 2022). Third, most studies lack dynamic decision-making and feedback optimization mechanisms, rendering them unable to actively adjust regional planning strategies based on prediction results to achieve closed-loop optimization and continuous improvement (Juárez-Varón & Juárez-Varón, 2024; Villalonga et al., 2021). Therefore, this study argues that a new model is needed—one that integrates multisource heterogeneous data, possesses strong spatiotemporal feature extraction capabilities, and can dynamically optimize planning strategies within a reinforcement learning (RL) framework.

Figure 1. Evaluating urban planning analysis methods

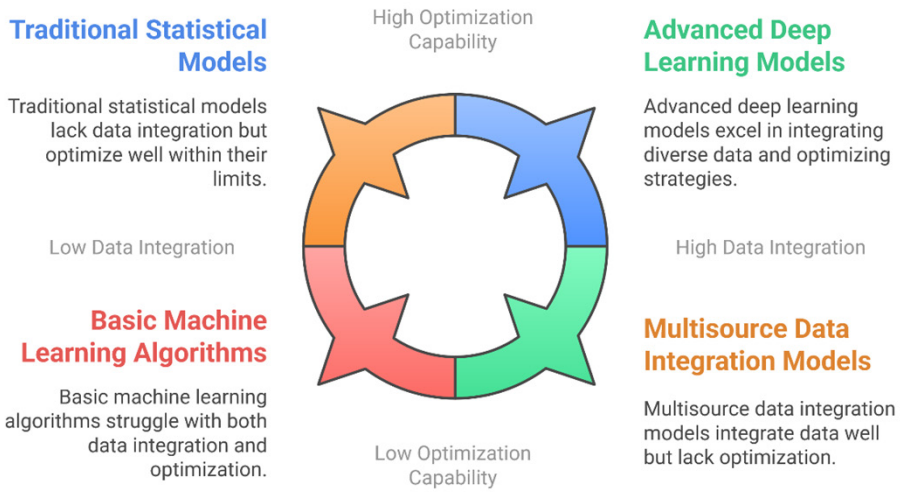

This article proposes a semantic web-enhanced RL-based urban planning optimization model (SWRL-UPOM), to optimize urban planning through precise prediction of spatiotemporal dynamics and iterative strategy refinement.

First, the model incorporated semantic web technologies to structure multisource data such as traffic and cultural activities, enabling efficient reasoning and dynamic data adaptation. The spatiotemporal adaptive multimodal graph convolutional network (STAMFGCN) was then designed to integrate multisource data and model complex relationships. By employing dynamic adaptive adjacency matrices and multi-scale graph convolution, STAMFGCN extracted topological features from multimodal data, such as traffic and cultural activities. Unlike static or single-perspective

approaches, it adjusted graph structures adaptively, based on planning actions and data changes, thereby capturing dynamic associations and enhancing predictive accuracy through complementary data integration.

Second, for fine-grained pollution prediction, the researchers introduced the spatiotemporal gated hierarchical attention long short-term memory network (STGHALSTM). This model combined spatial gating and hierarchical attention mechanisms with long short-term memory (LSTM) networks to emphasize critical spatiotemporal segments, dynamically weight features, and improve prediction precision and stability within complex correlations.

Finally, prediction results from STAMFGCN and STGHALSTM were integrated into a RL framework, where agents explored regional planning strategies and used pollution predictions as feedback. This closed-loop system iteratively optimized strategies, dynamically adjusting environmental conditions and enabled continuous improvement over static prediction-based methods. In summary, the contributions made to the field from this study are as follows:

- Researchers proposed STAMFGCN, which innovatively employed dynamic adjacency matrices and multi-scale convolution mechanisms to precisely capture the spatiotemporal dynamics of multimodal data. This offers the potential to significantly enhance the modeling capability of urban traffic networks and the accuracy of pollution predictions.
- Researchers designed STGHALSTM, which integrated spatial gating and spatiotemporal hierarchical attention mechanisms. This strengthened its modeling capabilities for the dynamic features of cultural activities and demonstrated higher prediction accuracy and robustness in noisy environments.
- Researchers integrated STAMFGCN and STGHALSTM into a proposed SWRL-UPOM, constructing a closed-loop dynamic optimization system to achieve intelligent, dynamic adjustments and continuous improvements in regional planning strategies.

The article is structured as follows. The Related Works section reviews past research. In Proposed Methodology, the SWRL-UPOM framework is presented, detailing its multi-component architecture, including STAMFGCN for spatial-temporal multimodal fusion, STGHALSTM for long-term trend prediction, and RL for adaptive urban policy optimization. The Experimental Setup describes the datasets, model configurations, and evaluation metrics used for performance assessment. The Results and Discussion section provides a comparative analysis of SWRL-UPOM against baseline models, demonstrating its advantages in urban decision-making and planning optimization. The Challenges and Future Directions section explores real-world deployment challenges, including data reliability, computational constraints, policy compliance, and stakeholder integration, while suggesting possible enhancements. Finally, the Conclusion summarizes key findings and outlines future research directions, such as scalability, hybrid RL strategies, and real-time urban data integration.

RELATED WORKS

Deep Learning-Based Urban Planning

With the acceleration of global urbanization, deep learning has become a key tool in urban planning, enabling complex spatiotemporal data analysis. Zhang et al. (2022) integrated nighttime light data, points of interest, and population migration data using the U-net network to achieve high-precision extraction of built-up areas in Guangzhou. While this improved accuracy, integrating diverse data introduced noise, therefore limiting its applicability in complex environments. Zhou et al. (2024) detection model, utilizing MobileBERT for feature extraction and CMA-ES for hyperparameter optimization, achieved 95% classification accuracy, demonstrating the effectiveness of evolutionary strategies in enhancing detection performance. This approach highlights the role of adaptive

optimization techniques, which aligns with this study's model and its use of RL for urban planning optimization.

Wang et al. (2022) developed a deep learning-based streetscape scoring model that analyzed street view images across six dimensions—such as aesthetics, safety, and vibrancy—providing insights into the relationship between street quality and components. However, its reliance on static images limited its capacity for capturing real-time urban dynamics. Juárez-Varón et al. (2024) conducted across Spain, Ecuador, Colombia, and Argentina, utilizing neurotechnology and qualitative research to analyze urban transport users' experiences. This research revealed that efficiency improvements in public transportation were the most valued CPS application.

In land-use configuration optimization, D. Wang et al. (2023b) used deep generative models with multi-head attention mechanisms for automated land-use generation but faced high computational costs for large-scale regions. Similarly, D. Wang et al. (2023a) leveraged generative adversarial networks for land-use planning, incorporating spatial graphs and migration data. Despite generating high-quality configurations, challenges remained in integrating multi-source heterogeneous data and ensuring practicality. Memos et al. (2018) review Internet of Things network architectures and security challenges, proposing the efficient algorithm for a media-based surveillance system, which integrated WSN security techniques with high-efficiency video coding for optimized packet routing and media compression. Experimental results demonstrated improved privacy protection, media security, and memory efficiency, aligning with the model in this study and its focus on secure, AI-driven urban planning where real-time data security and resource efficiency are critical.

Wang and Cao (2021) reviewed the extensive applications of deep learning in urban computing, highlighting the importance of multimodal data integration and spatiotemporal feature extraction while noting limitations in handling high-dimensional data and dynamic optimization. Assessing industrial energy consumption requires handling uncertainties in decision-making, which B. Wang et al. (2024) addressed using interval type-2 fuzzy sets and social network-based decision-maker analysis. Fang et al. (2022) introduced a deep neural network method, guided by planning principles, to generate realistic street networks by integrating professional knowledge. Despite its potential, this approach requires optimization for large-scale and real-time applications. Ren et al. (2023) proposed an improved support vector machine model for risk assessment in urban railway investment, enhancing accuracy through kernel functions and fuzzy membership design. The model constructed a robust risk index system using fuzzy sets and statistical methods, achieving high precision with minimal relative error in assessments.

RL-Based Urban Planning

Despite significant progress in applying deep learning to urban planning, challenges remain in managing complex decision-making, dynamic changes, and multi-stakeholder collaboration. RL has emerged as a promising approach for dynamic optimization and multi-objective balancing (Peng et al., 2021). Cao et al. (2024) proposed EPSSNet, a lightweight segmentation model integrating semantic flow branching, edge flow branching, and self-adapting weighting fusion, to enhance boundary-aware segmentation.

Qian et al. (2023) applied multi-agent RL to participatory planning, using spatial graphs and graph neural networks to enable stakeholders to vote on land-use types. While effective for stakeholder engagement, it struggled with computational efficiency and balancing interests in large-scale environments. Gupta et al. (2023) introduced a deep learning-based intrusion detection system, integrating convolutional neural networks (CNNs) and gated recurrent units to capture spatial and sequential patterns in network traffic data for smart cities. Adibhesami et al. (2024) integrated RL with multi-objective optimization to address public health emergencies and sustainable development, balancing health, economic, and environmental goals in simulations. However, practical applications required extensive parameter tuning, reducing flexibility in dynamic settings. Nie et al. (2022) proposed a spatial-temporal gated graph attention network, combining graph attention networks for

spatial learning, and gated recurrent units for temporal feature extraction for smart cities. Malik et al. (2023) proposed an automated urban waste classification model using CNNs, leveraging transfer learning and fine-tuning of pre-trained models. This approach enabled cost-effective and scalable waste management solutions, supporting smart city developments through efficient litter categorization. Gaurav et al. (2024) proposed a Chi-square feature selection method combined with JADE-based hyperparameter optimization for a CNN-based phishing detection model. This aligns with the model outlined in this study, with its focus on AI-driven optimization techniques for enhancing adaptive decision-making in urban planning.

In spatial optimization and facility placement, Liang et al. (2024) introduced SpoNet, and S. Wang et al. (2023) developed DeepMCLP, framing site selection as Markov decision processes to solve problems like *p*-median and *p*-center. These models improved speed and accuracy but faced challenges in real-time adjustments and large-scale data processing. Han et al. (2021) utilized RL with deep deterministic policy gradient to automate urban design, generating realistic building layouts that balance lighting and aesthetics. While promising, it required further optimization for large-scale and dynamic applications. Kakade et al. (2024) proposed a customized communication protocol for cloudlets, addressing power, memory constraints, fault tolerance, and task affinity to improve network efficiency. This aligns with this study's focus on real-time adaptive decision-making, where efficient network communication and resource optimization are critical for smart city and urban planning applications.

Ye et al. (2021) dynamically allocated road resources with RL, adapting to changing pedestrian and vehicle demands. However, scalability and adaptability in complex traffic networks remained areas for improvement. Upadhyay et al. (2024) explored role-based and attribute-based access control, blockchain-based authentication, and adaptive access control strategies, addressing privacy concerns, legal implications, and security risks. Li et al. (2023) introduced an identity-based privacy protection algorithm for secure cloud data access, leveraging a lattice-based strong forward secure signature scheme. That approach ensured robust user authentication and enhanced both forward and backward security for cloud computing environments.

Compared to existing methods, the proposed SWRL-UPOM achieved efficient integration of multi-source spatiotemporal data and dynamic optimization, by combining the STAMFGCN and the STGHALSTM, with the introduction of a RL mechanism. Tan et al. (2022) proposed the temporal and spatial momentum-based iteration gradient sign method to enhance the transferability of adversarial attacks against DNN-based speaker recognition systems. By leveraging gradient information from sample neighborhoods and interior spaces, the method outperformed existing attacks in both white-box and black-box scenarios.

METHOD

Current urban planning faces challenges in integrating multimodal data and optimizing strategies in real time. This study proposed a decision-making model to address these issues, the specific model flow is shown in Figure 2 and Algorithm 1.

Figure 2. Overall process diagram of the semantic web-enhanced reinforcement learning-based urban planning optimization model

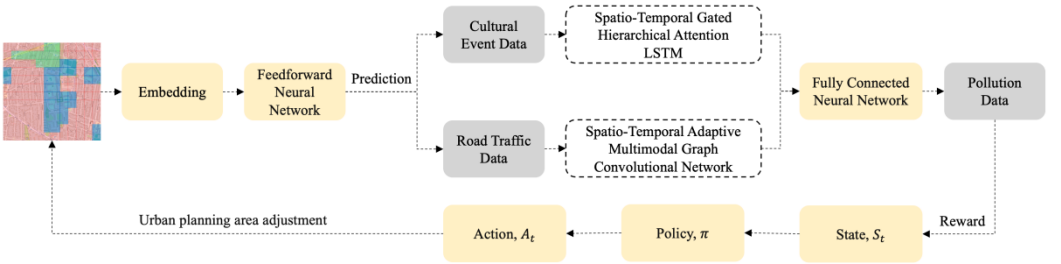

Note. LSTM = long short-term memory.

The urban region M was divided into grids, with spatial features X_i and temporal data T_t extracted for each grid cell. A fully connected neural network predicted road traffic R and cultural activity C, while STAMFGCN and STGHALSTM extracted spatiotemporal features from R and C. These features were fused to predict pollution P. An RL framework iteratively optimized planning actions based on P, reducing pollution while balancing urban functionality.

The predictions for R and C were computed as Equation (1):

$$\hat{R}_{i,t} = W_R^o h^L + b_R^o, \hat{C}_{i,t} = W_C^o h^L + b_C^o \quad (1)$$

Algorithm 1 Semantic Web-Enhanced Reinforcement Learning-Based Urban Planning Optimization Model

Step 1: Initialize Environment
- Initialize urban region M into grid cells with features X_i and T_t
- Initialize policy π with random weights
- Initialize reinforcement learning parameters

Step 2: Predict Road Traffic and Cultural Activity

For each time step t:
- R_pred = fully_connected_*NN* (X_i, T_t) # Equation (1)
- Cyprid = fully_connected_*NN* (X_i, T_t)

Step 3: Extract Spatiotemporal Features
- Traffic_Features = STAMFGCN (R_pred) # Equation (5)—multimodal graph convolution
- Event_Features = STGHALSTM (C_pred) # Equations (3) and (4)—attention-based LSTM

Step 4: Pollution Prediction
- Urban_Features = concatenate (Traffic_Features, Event_Features)
- P_pred = fully_connected_*NN* (Urban_Features) # Equation (12)

Step 5: Reinforcement Learning for Policy Optimization
- S_t = {P_pred, R_pred, C_pred, M} # current state representation
- A_t = select_action (π, S_t) # select urban planning action
- Execute (A_t) # apply action to adjust urban layout, traffic rules, etc.

Step 6: Compute Reward Function
- ΔP = P_pred_new - P_pred if ΔP < 0:
- R_t = λ * (ΔP)^(-1) # reward for pollution reduction else:
- R_t = -μ * ΔP # penalty for pollution increase # Equation (8)

Step 7: Update Policy Using Policy Gradient
- π = update_policy (π, S_t, A_t, R_t) # Equations (9) and (10)

Step 8: Train Model Using Multi-Objective Loss
- L_MSE = compute_MSE_loss (R_pred, C_pred, P_pred) # Equation (12)
- L_RL = compute_RL_loss (π, R_t) # Equation (13)
- L_Total = L_MSE + L_RL # Equation (16)

Step 9: Repeat Until Convergence
- Repeat steps 2–8 until optimal policy is learned

Step 10: Deploy Optimized Urban Planning Strategy
- Return Optimized_Strategy(A_t)

STGHALSTM

To capture the potential spatiotemporal dynamic features of cultural activity data $\hat{C}_{i,t}$, the authors designed the STGHALSTM. This model introduced two innovative modules on top of the traditional LSTM network: a spatial gating mechanism and a hierarchical attention mechanism. Both mechanisms aimed at better capturing spatiotemporal correlations and key features.

Traditional LSTMs primarily model temporal sequences using forget gates, input gates, and output gates. They cannot address, however, differences in the spatial dimension, such as the significantly varying impacts of traffic flow and cultural activities on pollution across different regions. Additionally, traditional LSTMs struggle to capture dynamic correlations between neighboring regions, such as the diffusion characteristics of pollutants between areas and the temporal variation of their influence intensities. To address this issue, a spatial gating mechanism was introduced into the LSTM structure, enabling the gating units to dynamically capture spatial influences in addition to temporal features. Specifically, for cultural activity data $\hat{C}_{i,t}$, the gating mechanism adjusted the state update process. The modified gating unit is described in Equation (2):

$$\begin{aligned} g_t &= \sigma\left(W_g X_t + U_g \hat{C}_{i,t} + b_g\right) \\ f_t &= \sigma\left(W_f X_t + U_f h_{t-1} + V_f g_t + b_f\right) \\ i_t &= \sigma\left(W_i X_t + U_i h_{t-1} + V_i g_t + b_i\right) \\ \tilde{c}_t &= \tanh\left(W_c X_t + U_c h_{t-1} + V_c g_t + b_c\right) \\ c_t &= f_t \odot c_{t-1} + i_t \odot \tilde{c}_t \\ o_t &= \sigma\left(W_o X_t + U_o h_{t-1} + V_o g_t + b_o\right) \end{aligned}, \tag{2}$$

Where, g_t was the gating signal that incorporates spatial features, W_g, U_g, V_f, V_i, V_c, and V_o were learnable parameters, b_g, b_f, b_i, b_c, and b_o were bias terms, σ represented the sigmoid activation function, and $\odot$ denoted element-wise multiplication.

Based on the obtained hidden state h_t, STGHALSTM further enhanced the capture of key spatiotemporal features, through a hierarchical attention mechanism. First, in the temporal dimension, the hidden states h_t, at different time steps, were dynamically weighted to emphasize critical time steps. The computation process is shown in Equation (3):

$$\alpha_t = \text{softmax}\left(\frac{h_t^{\top} W_t h_{t-1}}{\sqrt{d_t}}\right), \tag{3}$$

Where W_t represented the learnable parameters for temporal attention, and d_t was the feature dimension in the temporal domain. After temporal weighting, the dynamically

aggregated temporal feature was obtained as $h_t^{time} = \alpha_t \odot h_t$. In the spatial dimension, the simultaneous computation process to capture the contribution of different spatial locations at the current time step is described in Equation (4):

$$\beta_t = \text{softmax}\left(\frac{h_t^{\text{time T}} W_s \hat{C}_{i,t}}{\sqrt{d_s}}\right), h_t^{\text{spatial}} = \beta_t \odot \hat{C}_{i,t}, \tag{4}$$

Where W_s represented the learnable parameters for spatial attention, and d_s was the feature dimension in the spatial domain. Finally, the temporal and spatial features were fused to obtain a new hidden state $h_t^{final} = h_t^{time} + h_t^{spatial}$. Lastly, the fused hidden state was mapped through a linear transformation layer to the potential spatiotemporal dynamic features of cultural activity data $\hat{C}_{i,t}$, as expressed by $F_C = \text{Linear}\left(h_t^{final}\right)$.

STAMFGCN

To address the modeling requirements of road traffic data $\hat{R}_{i,t}$ in complex spatial topologies and temporal dynamics, this study proposed the STAMFGCN. Compared with traditional graph convolutional networks (GCNs), STAMFGCN introduced a dynamic adaptive adjacency matrix and a multi-scale convolution mechanism, significantly enhancing its ability to extract features from dynamic traffic data and improving the modeling accuracy of complex spatiotemporal relationships.

In STAMFGCN, the spatial units of the urban region were represented as a graph structure, with the node set $\{cell_i\}_{i=1}^{G}$, where each node corresponded to a spatial grid cell $cell_i$, and its features included road traffic-related data. The connectivity of the graph was modeled by a dynamic adjacency matrix A_t, where the element $(A_t)_{ij}$ represented the dynamic association strength between node i and node j at time step t. The multi-scale convolution computation of STAMFGCN is shown in Equation (5):

$$H^{(l+1)} = \text{BatchNorm}\left(\sigma\left(\sum_{k=1}^{K} \alpha_k^{(l)} \widetilde{D}_t^{-\frac{1}{2}} \widetilde{A}_t^k \widetilde{D}_t^{-\frac{1}{2}} H^{(l)} W_k^{(l)}\right) + H^{(l)}\right), \tag{5}$$

Where $\widetilde{A}_t = A_t + I$ represented the adjacency matrix with self-loops added, where II was the identity matrix, ensuring that each node could aggregate its own features. $\widetilde{D}_t$ was the degree matrix of $\widetilde{A}_t$. $\widetilde{A}_t^k$ denoted the k-th power of the adjacency matrix, which captured multi-scale topological relationships between nodes. K was the maximum neighborhood scale for the convolution operation, and $\alpha_k^{(l)}$ was the attention weight at layer l, dynamically adjusting the contribution of different neighborhood scales. $H^{(l)}$ represented the node feature representation at layer l, and $W_k^{(l)}$ was the corresponding learnable parameter matrix. The non-linear activation function was $ReLU$. The computation of $\alpha_k^{(l)}$ is described in Equation (6):

$$\alpha_k^{(l)} = \text{softmax}\left(W_\alpha^{(l)} \cdot H^{(l)}\right). \tag{6}$$

Unlike the fixed adjacency matrix in traditional GCNs, A_t could be dynamically adjusted, based on the current time step's node features and historical states, to account for the influence of spatiotemporal changes on internode relationships. The computation process is shown in Equation (7):

$$A_t = \sigma\left(Linear\left(\left[H_R \parallel A_t^{\text{prev}}\right]\right)\right), \tag{7}$$

Where H_R represented the embedded traffic data features at the current time step, and A_t^{prev} was the adjacency matrix from the previous time step. Through this mechanism, STAMFGCN

dynamically adjusted connection strengths, based on the current time step's node features, enabling the model to capture real-time changes in traffic patterns, such as the impact of peak-hour traffic surges on surrounding nodes. This enhanced the accuracy of spatiotemporal relationship modeling. Finally, after L layers of graph convolution, the dynamic features of road traffic data $\hat{R}_{i,t}$ were output as $F_R = Linear(H^L)$.

After obtaining the potential spatiotemporal dynamic features F_C of cultural activity data $\hat{C}_{i,t}$ and the dynamic features F_R of road traffic data $\hat{R}_{i,t}$, the two were concatenated as $F_{Fusion} = Concat(F_C, F_R)$. F_{Fusion} was then used as the input to a fully connected neural network to predict the final pollution data as $\hat{P}_{i,t} = Linear(F_{Fusion})$.

RL

To dynamically optimize regional planning and reduce pollution, the pollution prediction $\hat{P}_{i,t}$ was integrated into a RL framework, forming a closed-loop decision-making system.

The RL framework consisted of an agent that select planning actions A_t, based on the current state S_t, which included pollution data $\hat{P}_{i,t}$, road traffic $\hat{R}_{i,t}$, cultural activities $\hat{C}_{i,t}$ and map information $M\left(S_t = \left\{\hat{P}_{i,t}, \hat{R}_{i,t}, \hat{C}_{i,t}, M\right\}\right)$. The policy network π_θ, parameterized by θ, output action probabilities, guiding adjustments such as modifying roads, increasing green spaces, or altering traffic signals.

Upon executing A_t, the environment updated $\hat{R}_{i,t+1}$ and $\hat{C}_{i,t+1}$, and predicted new pollution levels $\hat{P}_{i,t+1}$. The pollution change $\Delta P = \hat{P}_{i,t+1} - \hat{P}_{i,t}$ defined the reward R_t, designed as Equation (8):

$$R_t = \begin{cases} \lambda \cdot (\Delta P_t)^{-1}, & \text{if } \Delta P_t < 0 \\ -\mu \cdot \Delta P_t, & \text{if } \Delta P_t \geq 0 \end{cases}, \tag{8}$$

Where λ and μ were weights for rewards and penalties. Positive rewards encouraged actions that reduce pollution, while penalties discourage harmful strategies.

The policy network π_θ was optimized via policy gradients, maximizing cumulative rewards (CRs) $J(\theta)$, as shown in Equation (9):

$$J(\theta) = \mathbb{E}_{\pi_\theta}\left[\sum_{k=0}^{\infty} \gamma^k R_{t+k}\right], \tag{9}$$

Where $\gamma \in (0, 1)$ was the discount factor used to balance the importance of future rewards. The update process for the policy gradient was expressed as shown in Equation (10):

$$\nabla_\theta J(\theta) = \mathbb{E}_{\pi_\theta}\left[\nabla_\theta \log \pi_\theta(A_t S_t) Q^\pi(S_t, A_t)\right], \tag{10}$$

Where $Q^\pi(S_t, A_t)$ was the action-value function. To approximate $Q^\pi(S_t, A_t)$, a Q-network $Q_\phi(S_t, A_t)$, parameterized by ϕ, minimized the Bellman error, as described in Equation (11):

$$\mathscr{L}_{value}(\phi) = \mathbb{E}_{(S_t, A_t, R_t, S_{t+1}) \sim \mathscr{D}}\left[\left(Q_\phi(S_t, A_t) - \left(R_t + \gamma \max_{A'} Q_{\phi'}(S_{t+1}, A')\right)\right)^2\right], \tag{11}$$

Where ϕ' represented the target network, periodically updated to stabilize training. The agent stores experienced (S_t, A_t, R_t, S_{t+1}) in a replay buffer, samples batches, and optimized Q_ϕ.

Simultaneously, π_θ updated θ using Q-values, to favor actions that maximized long-term rewards, with updates $\theta \leftarrow \theta + \alpha \nabla_\theta J(\theta)$, where α was the learning rate.

Semantic Web-Enhanced RL Model

The proposed semantic web-enhanced RL model leveraged semantic web technologies to structure and integrate heterogeneous data sources, such as traffic patterns, pollution levels, and cultural activities, into a unified knowledge graph. This structured representation enabled semantic reasoning and dynamic data linkage, ensuring that contextually relevant insights were extracted for urban planning decisions. By using ontologies and SPARQL queries, the model enhanced interpretability and supported efficient querying of complex, multi-relational datasets. This semantic enrichment facilitated better understanding of interdependencies in urban environments, providing a robust foundation for RL to optimize planning strategies dynamically. The integration of semantic web technologies ensured adaptability and scalability, making the framework suitable for diverse urban scenarios.

Loss Function and Training Strategy

To optimize the proposed SWRL-UPOM, multiple loss functions were defined. Specifically, these included mean squared error (MSE) loss functions for predicting road traffic data R, cultural activity data C, and pollution data P, as well as a loss function for policy optimization in the RL framework.

First, for each grid cell $cell_i$ at time step t, the model predicted road traffic data $\hat{R}_{i,t}$, cultural activity data $\hat{C}_{i,t}$, and pollution data $\hat{P}_{i,t}$. The MSE loss function was computed as shown in Equation (12):

$$\mathscr{L}_{MSE} = \frac{1}{N}\sum_{i=1}^{N}\left(\| \hat{R}_{i,t} - R_{i,t}\|^2 + \| \hat{C}_{i,t} - C_{i,t}\|^2\right) + \| \hat{P}_{i,t} - P_{i,t}\|^2, \tag{12}$$

Where N was the number of samples, and $R_{i,t}$, $C_{i,t}$, and $P_{i,t}$ represented the actual road traffic data, cultural activity data, and pollution data, respectively.

In the RL framework, the design of the loss function aimed to optimize the agent's policy, enabling it to select optimal regional planning actions in a dynamic environment to maximize CRs. The RL loss function included the policy loss, value loss, and entropy regularization term. The computation process is shown in Equation (13):

$$\mathscr{L}_{RL} = \mathscr{L}_{\text{policy}} + c_1 \mathscr{L}_{\text{value}} - c_2 \mathscr{H}, \tag{13}$$

Where $\mathscr{L}_{\text{policy}}$ represented the policy loss, which was used to maximize CRs, and $\mathscr{L}_{\text{value}}$ represented the value loss, which ensured accurate estimation of the state-action value function. $\mathscr{H}$ was the entropy regularization term, designed to encourage exploration in the policy. c_1 and c_2 were hyperparameters used to balance the weights of different loss components. Specifically, the computation process for the policy loss $\mathscr{L}_{\text{policy}}$ was described in Equation (14):

$$\mathscr{L}_{\text{policy}} = -\mathbb{E}_{\pi_\theta}\left[\log \pi_\theta(A_t S_t)\, Q^{\pi}(S_t, A_t)\right], \tag{14}$$

Where $\pi_\theta(A_t S_t)$ denoted the probability of selecting action A_t in state S_t, and $Q^{\pi}(S_t, A_t)$ represented the state-action value function, which evaluated the expected CR obtained by taking action A_t in state S_t. This term encouraged the agent to select actions that yielded high rewards, by maximizing the probability distribution output by the policy network.

In addition, the computation process for the value loss $\mathscr{L}_{\text{value}}$ is shown in Equation (11), and the computation process for the entropy regularization term $\mathscr{H}$ is shown in Equation (15):

$$\mathscr{H} = -\mathbb{E}_{\pi_\theta}\left[\sum_{a} \pi_\theta(a S_t)\log \pi_\theta(a S_t)\right]. \tag{15}$$

Combining the above components, the overall loss function of the model was designed as shown in Equation (16):

$$\mathcal{L} = \mathcal{L}_{MSE} + \mathcal{L}_{RL}. \tag{16}$$

RESULTS AND ANALYSIS

Experimental Environment and Settings

To verify the effectiveness of the proposed SWRL-UPOM, all model training and testing was conducted on a server equipped with an Intel Xeon E5 series multi-core central processing unit, 64GB memory, and an NVIDIA GeForce RTX 4090 24GB graphics processing unit. The operating system used was Ubuntu 20.04, with Python 3.8 and PyTorch 1.12 as the primary deep learning development environment.

For hyperparameter settings, the fully connected neural network was configured with three hidden layers, each containing 256 hidden units. The STAMFGCN was set to two layers, while the STGHALSTM was set to four layers. The optimizer used was Adam, with an initial learning rate fixed at 10^{-4}, and a step decay strategy was applied based on the loss curve to ensure smoother model convergence. The batch size was set to 32, with data randomly sampled in each batch for training. In the RL component, the discount factor γ was set to 0.95 to balance short-term and long-term rewards. The positive and negative reward coefficients λ and μ were set to 0.5 and 1.0, respectively, to regulate the agent's incentive intensity for pollution reduction and increase.

Dataset and Evaluation Metrics

The City Pulse EU FP7 dataset was utilized as the foundation, integrating road traffic data, pollution data, cultural activity announcements, and urban region annotations from OpenStreetMap. Specifically, the vehicle traffic data collection spanned six months, covering flow, speed, and other information across multiple observation points, totaling 449 locations. Pollution data was simulated and integrated using the Air Quality Index and traffic sensor locations, also covering 449 observation points. The cultural activity data was sourced from event announcements in the city of Aarhus, providing information on the frequency and types of cultural events in various urban regions. By merging road traffic data, cultural activity data, and pollution data, and combining them with OpenStreetMap's regional annotations, the multimodal spatiotemporal characteristics within different urban grid cells was represented comprehensively.

To evaluate the model's spatiotemporal prediction and dynamic decision-making performance in an urban environment, the following two commonly used evaluation metrics were selected. MSE evaluated the prediction accuracy of the model for road traffic, cultural activities, and pollution data. It measured the average squared difference between predicted values and actual values, reflecting the model's deviation. CR measured the total rewards obtained by the agent during sequential decision-making in the RL component. It served as a core standard for evaluating the quality of planning strategies. Sustained accumulation of positive rewards indicated that the agent's decision-making capabilities for reducing pollution and maintaining urban functionality were continuously improving, whereas negative feedback prompted the agent to make adjustments in subsequent training iterations.

EXPERIMENTAL RESULTS

Ablation Study

To validate the effectiveness of the components in the proposed method, an ablation study was conducted. In this study, STAMFGCN and STGHALSTM were sequentially removed, and the RL

framework evaluated the contribution of each component regarding improving model performance. The experimental results are presented in Table 1.

Table 1. Impact of individual components of semantic web-enhanced reinforcement learning-based urban planning optimization model on model performance

Methods	Mean Squared Error	Cumulative Reward
Baseline (FNN)	11.32	-
FNN+STAMFGCN	8.47	-
FNN+STGHALSTM	7.96	-
FNN+STAMFGCN+STGHALSTM	5.24	-
SWRL-UPOM	5.10	16.42

Note. FNN = fully connected neural network; STAMFGCN = XX; STGHALSTM = XX; SWRL-UPOM = semantic web-enhanced reinforcement learning-based urban planning optimization model.

Experimental results showed that using only the fully connected neural network for pollution prediction resulted in high MSE (11.32), and no decision-making benefits. Adding STAMFGCN significantly reduced MSE by capturing spatial dependencies in road traffic data, thereby demonstrating the effectiveness of the spatiotemporal adaptive adjacency matrix. Incorporating STGHALSTM further improved performance by modeling spatiotemporal dynamics in cultural activity data through spatial gating and hierarchical attention mechanisms. While STAMFGCN and STGHALSTM individually enhanced performance, their combination achieved the best results, highlighting their complementarity in handling multimodal data. Integrating RL into the SWRL-UPOM model maintained prediction accuracy with slight MSE changes but introduced substantial CR, enabling adaptive updates to planning strategies, based on pollution feedback. These findings underscored the importance of STAMFGCN and STGHALSTM for multimodal spatiotemporal analysis and the RL framework for dynamic decision-making.

Hyperparameter Experiments

To further investigate the impact of hyperparameter settings on model performance, multiple tests were conducted focusing on the discount factor γ and the positive and negative reward coefficients λ and μ. These experiments were designed to examine the effects of these parameters on balancing model prediction and decision-making performance. The experimental results are shown in Figure 3.

Figure 3. Experimental results

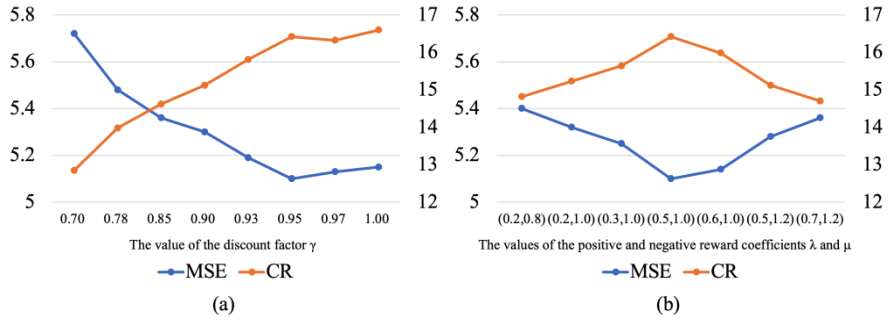

Note. (a) shows the impact of the discount factor γ on model performance; (b) shows the impact of positive and negative reward coefficients λ and μ on model performance. MSE = mean squared error; CR = cumulative reward.

It can be observed that when γ was set too low, the agent focused more on short-term rewards, often failing to accumulate sufficient long-term CR; this resulted in noticeably lower CR and a slight decrease in pollution prediction accuracy. As γ increased, the model gradually emphasized long-term returns, leading to an increase in CR, while maintaining optimal MSE levels. However, if γ reached 1.00, it implies the agent gave infinite priority to future returns. While this may theoretically result in higher CR, in practice, it may lead to slower convergence or instability during training, due to excessively long sequences. Overall, the choice of γ should match the duration and focus of the specific urban planning task: too low, and it results in suboptimal short-term rewards; too high, and it may slow convergence or cause instability. In most scenarios, γ values between 0.90 and 0.97 struck a balance between prediction and decision-making performance. In this experiment, γ was set to 0.95.

Additionally, when λ was too small, the model provided insufficient incentives for pollution reduction, resulting in relatively low CR because the agent could not fully exploit the positive rewards from reducing pollution. On the other hand, was λ too large, the model may have overly prioritized pollution reduction rewards, neglecting balance in other aspects. When μ was set too high, the penalty for pollution increase became severe, which may have suppressed pollution violations to some extent, but may have caused the agent to fall into excessive penalties during the early training stages, leading to reduced CR. Overall, $\lambda = 0.5$ and $\mu = 1$ provided relatively ideal performance for MSE and CR, maintaining good accuracy in pollution prediction while providing appropriate positive and negative feedback intensities for the RL-based planning decisions.

Module Comparison Experiment

A module comparison experiment was conducted to further validate the effectiveness of the proposed modules. In this experiment, STAMFGCN and STGHALSTM were replaced with other mainstream methods, such as standard GCN or GraphSAGE, and basic LSTM. The experimental results are presented in Table 2.

Table 2. Results of the module comparison experiment for spatiotemporal adaptive multimodal graph convolutional network and spatiotemporal gated hierarchical attention long short-term memory network

Module Combination	Mean Squared Error	Cumulative Reward
GCN (Kipf & Welling, 2016) +LSTM (Graves, 2012)	6.18	14.02
GraphSAGE (Hamilton et al., 2017) +LSTM	6.03	14.39
STAMFGCN+LSTM	5.51	15.33
GCN+STGHALSTM	5.43	15.56
GraphSAGE+ STGHALSTM	5.37	15.71
STAMFGCN+STGHALSTM	5.10	16.42

Note. GCN = graph convolutional network; LSTM = long short-term memory; STAMFGCN = spatiotemporal adaptive multimodal graph convolutional network; STGHALSTM = spatiotemporal gated hierarchical attention long short-term memory network.

It could be observed that using STAMFGCN and STGHALSTM achieved optimal performance on both MSE and CR metrics (MSE: 5.10, CR: 16.42). Specifically, the dynamic adaptive adjacency matrix in STAMFGCN not only effectively captured road traffic changes in real-time but also utilized attention mechanisms in multi-scale convolution to highlight key neighborhoods, making it superior to traditional GCN or GraphSAGE in urban topology modeling. STGHALSTM, through spatial gating and hierarchical attention mechanisms, enabled more precise modeling of the spatiotemporal dependencies of cultural activities, outperforming basic LSTM by better emphasizing critical moments and spatial regions. The integration of these two modules, under the RL framework, resulted in more accurate pollution predictions and superior planning decisions. These findings demonstrated that the proposed modules' innovations in multimodal fusion and spatiotemporal dependency modeling contributed to performance gains.

Efficiency Experiment

An efficiency experiment was conducted to evaluate how straightforward it might be to deploy the proposed model. In this experiment, the training and inference efficiency of different methods was examined under identical hardware and hyperparameter settings. Metrics included the number of training epochs completed per second, the training time per batch, and the inference time for a single test sample. The experimental results are presented in Table 3.

Table 3. Efficiency comparison results of different models

Methods	Epoch (seconds)	Batch Time (minutes)	Inference Time (minutes)
GCN+LSTM	0.61	58.43	0.38
GraphSAGE+LSTM	0.58	59.30	0.41
SWRL-UPOM	0.48	72.86	0.49

Note. GCN = graph convolutional network; LSTM = long short-term memory; SWRL-UPOM = a semantic web-enhanced reinforcement learning-based urban planning optimization model.

In terms of training and inference times, SWRL-UPOM achieved the fastest epoch time (0.48 seconds), but had a slightly higher batch time (72.86 minutes), and inference time (0.49 minutes), indicating a trade-off between overall training efficiency and computational complexity, due to its advanced spatiotemporal modeling and RL framework. This was mainly due to its integration of

multiple mechanisms, including the dynamic adaptive adjacency matrix, multi-head attention, and RL-based decision-making, which led to a more complex network structure and additional graphics processing unit computation and memory overhead. Previous experiments demonstrate, however, that SWRL-UPOM significantly outperformed other methods in terms of spatiotemporal modeling and dynamic strategy optimization. The additional time cost proved justified and worthwhile. For GCN+LSTM and GraphSAGE+LSTM, the network structures were relatively simpler, allowing for more training epochs per second and shorter inference times per sample. However, due to the lack of adaptive graph structures or RL frameworks, they struggled to achieve higher pollution prediction accuracy and dynamic decision-making benefits in complex urban planning tasks.

State-of-the-Art Comparison Experiment

To validate the effectiveness of SWRL-UPOM in urban planning optimization, it was compared with four state-of-the-art methods, as shown in Table 4. Table 4 presents a comparative analysis of SWRL-UPOM against existing state-of-the-art methods, evaluating MSE and CR. SWRL-UPOM achieved the lowest MSE (5.10), and highest CR (16.42), surpassing prior models in both pollution prediction accuracy and dynamic urban optimization efficiency. The STAMFGCN and STGHALSTM modules were unchanged regarding predicting traffic, cultural activity, and pollution data, with the primary difference being the inclusion of the RL-based decision update mechanism.

Table 4. Comparison results between semantic web-enhanced reinforcement learning-based urban planning optimization model and existing state-of-the-art methods

Methods	Mean Squared Error	Cumulative Reward
D. Wang et al. (2023b)	5.72	14.68
D. Wang et al. (2023a)	5.60	15.02
D. Wang et al. (2020)	5.54	14.92
Sun and Dogan (2023)	5.48	15.22
SWRL-UPOM	5.10	16.42

Note. SWRL-UPOM = a semantic web-enhanced reinforcement learning-based urban planning optimization model.

SWRL-UPOM outperformed all four methods in the CR metric, demonstrating its ability to improve planning strategies iteratively through RL. By integrating environmental feedback, SWRL-UPOM achieved superior dynamic decision-making that balanced urban functionality and environmental needs.

D. Wang et al. (2023a, 2023b) employed deep generative approaches for land-use configuration but faced challenges. D. Wang et al. (2023a) struggled with modeling hierarchical dependencies and interactions between functional zones, leading to inconsistencies in scenarios with intensive urban interactions. D. Wang et al. (2023b) introduced adversarial learning, but found this was less effective with continuous data like traffic and pollution, thus limiting its capacity for real-time updates. In contrast, SWRL-UPOM integrated RL with STAMFGCN and STGHALSTM, creating a closed-loop planning-feedback-optimization system. STAMFGCN captured spatiotemporal dependencies in road networks, while STGHALSTM modeled cultural activity-pollution interactions. This synergy enabled adaptive strategy updates and precise pollution regulation, overcoming the limitations of D. Wang et al. (2023a, 2023b).

To demonstrate practical effectiveness, re-planned regions and pollution heatmaps were visualized (Figure 4). D. Wang et al. (2023b) improved functional zone organization but localized green spaces, limiting pollution isolation. D. Wang et al. (2023a) distributed

functional zones more evenly, but pollution control remained insufficient. D. Wang et al. (2020) slightly increased green space distribution but failed to address high-risk pollution areas effectively. Sun and Dogan (2023) optimized green space distribution using multi-objective strategies but achieved limited pollution mitigation for residential areas.

Figure 4. Visualization comparison of regional planning re-optimized by different models

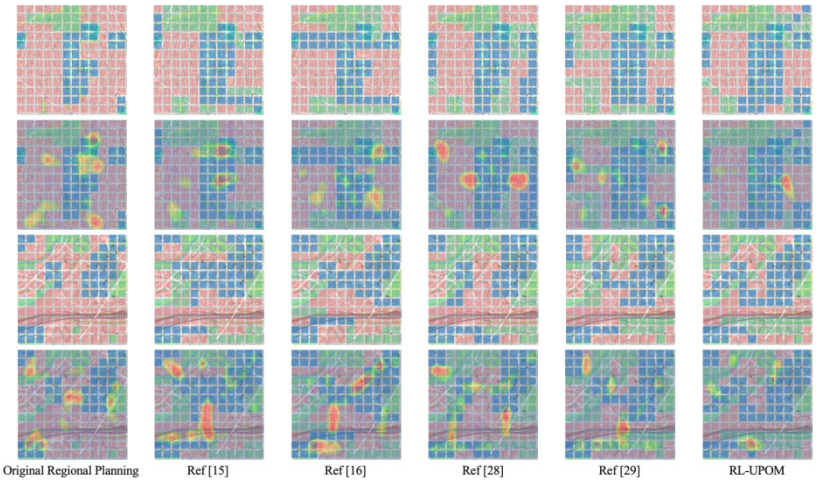

Note. RL-UPOM = XX.

SWRL-UPOM showed clear advantages in zoning and pollution distribution. It refined residential and commercial boundaries, strategically placed green spaces around pollution sources, and reduced high-pollution zones while controlling diffusion trends. These results highlight SWRL-UPOM's capability for dynamic optimization and precise pollution regulation through RL.

CONCLUSION

To address challenges in multi-source data integration, dynamic optimization, and complex spatiotemporal modeling in urban planning, the authors of this study proposed the SWRL-UPOM. By integrating semantic web technologies, the STAMFGCN, STGHALSTM, and RL enabled efficient multimodal spatiotemporal modeling and dynamic optimization. STAMFGCN captured dynamic traffic and spatial structures, STGHALSTM enhanced spatiotemporal sequence analysis, and the semantic web facilitates structured data integration—all of which supported intelligent decision-making. Experimental results show that SWRL-UPOM achieved a MSE of 5.10, outperforming baseline models, and attained a CR of 16.42, demonstrating its superior adaptability in optimizing urban planning strategies. However, SWRL-UPOM faces limitations, including high resource demands, simplistic reward design, and insufficient handling of multi-objective scenarios and multi-agent collaboration. Future work will address these issues by introducing multi-objective optimization, multi-agent mechanisms, and improved computational efficiency, as well as exploring cross-regional and multi-scenario applications to enhance its generalization and practical deployment in urban planning.

CONFLICTS OF INTEREST

We wish to confirm that there are no known conflicts of interest associated with this publication and there has been no significant financial support for this work that could have influenced its outcome.

FUNDING STATEMENT

No funding was received for this work.

PROCESS DATES

March 7, 2025
Received: January 23, 2025, Revision: February 25, 2025, Accepted: February 25, 2025

CORRESPONDING AUTHOR

Correspondence should be addressed to Jun Zhang (China, 13704515827@126.com)

REFERENCES

Adibhesami, M. A., Karimi, H., & Sepehri, B. (2024). Optimizing urban design for pandemics using reinforcement learning and multi-objective optimization. In Cheshmehzangi, A., Batty, M., Allam, Z., & Jones, D. S. (Eds.), *City information modelling* (pp. 77–94). Springer., DOI: 10.1007/978-981-99-9014-6_5

Alem, A., & Kumar, S. (2022). Transfer learning models for land cover and land use classification in remote sensing image. *Applied Artificial Intelligence*, *36*(1), 2014192. DOI: 10.1080/08839514.2021.2014192

Bai, H., Li, Z., Guo, H., Chen, H., & Luo, P. (2022). Urban green space planning based on remote sensing and geographic information systems. *Remote Sensing (Basel)*, *14*(17), 4213. DOI: 10.3390/rs14174213

Cao, Z., Villafuerte, G. Z., & Almaznaai, J. (2024). EPSSNet: A lightweight network with edge processing and semantic segmentation for mobile robotics. *International Journal on Semantic Web and Information Systems*, *20*(1), 1–22. DOI: 10.4018/IJSWIS.342087

Dowlatshahi, M. B., Rafsanjani, M. K., & Gupta, B. B. (2021). An energy aware grouping memetic algorithm to schedule the sensing activity in WSNs-based IoT for smart cities. *Applied Soft Computing*, *108*, 107473. DOI: 10.1016/j.asoc.2021.107473

Fang, Z., Jin, Y., & Yang, T. (2022). Incorporating planning intelligence into deep learning: A planning support tool for street network design. *Journal of Urban Technology*, *29*(2), 99–114. DOI: 10.1080/10630732.2021.2001713

Gaurav, A., Chui, K. T., Arya, V., Attar, R. W., Bansal, S., Alhomoud, A., & Psannis, K. (2024). Optimized AI-driven semantic web approach for enhancing phishing detection in e-commerce platforms. *International Journal on Semantic Web and Information Systems*, *20*(1), 1–13. DOI: 10.4018/IJSWIS.359767

Gokasar, I., Pamucar, D., Deveci, M., Gupta, B. B., Martinez, L., & Castillo, O. (2023). Metaverse integration alternatives of connected autonomous vehicles with self-powered sensors using fuzzy decision making model. *Information Sciences*, *642*, 119192. DOI: 10.1016/j.ins.2023.119192

Graves, A. (2012). *Supervised sequence labelling with recurrent neural networks*. Springer., DOI: 10.1007/978-3-642-24797-2

Gupta, B. B., Chui, K. T., Gaurav, A., Arya, V., & Chaurasia, P. (2023). A novel hybrid convolutional neural network-and gated recurrent unit-based paradigm for IoT network traffic attack detection in smart cities. *Sensors (Basel)*, *23*(21), 8686. DOI: 10.3390/s23218686 PMID: 37960386

Hamilton, W., Ying, Z., & Leskovec, J. (2017). Inductive representation learning on large graphs. In *Proceedings of the 31st International Conference on Neural Information Processing Systems (NIPS'17)* (pp. 1025–1035). Curran Associates Inc.

Han, Z., Yan, W., & Liu, G. (2021). A performance-based urban block generative design using deep reinforcement learning and computer vision. In *Proceedings of the 2020 DigitalFUTURES: The 2nd International Conference on Computational Design and Robotic Fabrication (CDRF 2020)* (pp. 134–143). Springer. DOI: 10.1007/978-981-33-4400-6_13

Juárez-Varón, D., Gaón, R. E. E., Mengual-Recuerda, A., & Vera-Sepúlveda, C. (2024). neurotechnologies applied to society's perception of cyber-physical systems (CPS) in smart cities. *International Journal on Semantic Web and Information Systems*, *20*(1), 1–32. DOI: 10.4018/IJSWIS.335947

Juárez-Varón, D., & Juárez-Varón, M. Á. (2024). SEO vs. UX in web design: Are companies' digital marketing strategies correct? A neurotechnological study. *International Journal of Software Science and Computational Intelligence*, *16*(1), 1–26. DOI: 10.4018/IJSSCI.342127

Kakade, M. S., Anupama, K. R., Nayak, S., & Garang, S. (2024). Custom network protocol stack for communication between nodes in a cloudlet system. *International Journal of Cloud Applications and Computing*, *14*(1), 1–24. DOI: 10.4018/IJCAC.339891

Khalil, U., Aslam, B., Azam, U., & Khalid, H. M. D. (2021). Time series analysis of land surface temperature and drivers of urban heat island effect based on remotely sensed data to develop a prediction model. *Applied Artificial Intelligence*, *35*(15), 1803–1828. DOI: 10.1080/08839514.2021.1993633

Kipf, T. N., & Welling, M. (2016). Semi-supervised classification with graph convolutional networks. *arXiv preprint arXiv:1609.02907*. DOI: 10.1109/LGRS.2018.2869563

Laurini, R. (2018). *Information systems for urban planning: A hypermedia cooperative approach*. CRC Press., DOI: 10.1201/9781315274713

Li, F., Wang, J., & Song, Z. (2023). Privacy protection of cloud computing based on strong forward security. *International Journal of Cloud Applications and Computing*, *13*(1), 1–9. DOI: 10.4018/IJCAC.323804

Liang, H., Wang, S., Li, H., Zhou, L., Chen, H., Zhang, X., & Chen, X. (2024). SpoNet: Solve spatial optimization problem using deep reinforcement learning for urban spatial decision analysis. *International Journal of Digital Earth*, *17*(1), 2299211. DOI: 10.1080/17538947.2023.2299211

Liu, Y., & Ye, M. (2023). Application and validity analysis of IoT in smart city based on entropy method. *Applied Artificial Intelligence*, *37*(1), 2166234. DOI: 10.1080/08839514.2023.2166234

Malik, M., Prabha, C., Soni, P., Arya, V., Alhalabi, W. A., Gupta, B. B., Albeshri, A. A., & Almomani, A. (2023). Machine learning-based automatic litter detection and classification using neural networks in smart cities. *International Journal on Semantic Web and Information Systems*, *19*(1), 1–20. DOI: 10.4018/IJSWIS.324105

Memos, V. A., Psannis, K. E., Ishibashi, Y., Kim, B. G., & Gupta, B. B. (2018). An efficient algorithm for media-based surveillance system (EAMSuS) in IoT smart city framework. *Future Generation Computer Systems*, *83*, 619–628. DOI: 10.1016/j.future.2017.04.039

Nie, X., Peng, J., Wu, Y., Gupta, B. B., & Abd El-Latif, A. A. (2022). Real-time traffic speed estimation for smart cities with spatial temporal data: A gated graph attention network approach. *Big Data Research*, *28*, 100313. DOI: 10.1016/j.bdr.2022.100313

Orieno, O. H., Ndubuisi, N. L., Ilojianya, V. I., Biu, P. W., & Odonkor, B. (2024). The future of autonomous vehicles in the US urban landscape: A review: Analyzing implications for traffic, urban planning, and the environment. *Engineering Science & Technology Journal*, *5*(1), 43–64. DOI: 10.51594/estj.v5i1.721

Peng, N., Xi, Y., Rao, J., Ma, X., & Ren, F. (2021). Urban multiple route planning model using dynamic programming in reinforcement learning. *IEEE Transactions on Intelligent Transportation Systems*, *23*(7), 8037–8047. DOI: 10.1109/TITS.2021.3075221

Puchol-Salort, P., O'Keeffe, J., van Reeuwijk, M., & Mijic, A. (2021). An urban planning sustainability framework: Systems approach to blue green urban design. *Sustainable Cities and Society*, *66*, 102677. DOI: 10.1016/j.scs.2020.102677

Qian, K., Mao, L., Liang, X., Ding, Y., Gao, J., Wei, X., Guo, Z., & Li, J. (2023). AI agent as urban planner: Steering stakeholder dynamics in urban planning via consensus-based multi-agent reinforcement learning. *arxiv preprint arxiv:2310.16772*. DOI: 10.1061/JUPDAJ.0000199

Ren, R., Fang, J., Hu, J., Ma, X., & Li, X. (2023). Risk assessment modeling of urban railway investment and financing based on improved SVM model for advanced intelligent systems. *International Journal on Semantic Web and Information Systems*, *19*(1), 1–19. DOI: 10.4018/IJSWIS.331596

Sharma, A., Singh, S. K., Chhabra, A., Kumar, S., Arya, V., & Moslehpour, M. (2023). A novel deep federated learning-based model to enhance privacy in critical infrastructure systems. *International Journal of Software Science and Computational Intelligence*, *15*(1), 1–23. DOI: 10.4018/IJSSCI.334711

Sun, Y., & Dogan, T. (2023). Generative methods for urban design and rapid solution space exploration. *Environment and Planning. B, Urban Analytics and City Science*, *50*(6), 1577–1590. DOI: 10.1177/23998083221142191

Tan, H., Gu, Z., Wang, L., Zhang, H., Gupta, B. B., & Tian, Z. (2022). Improving adversarial transferability by temporal and spatial momentum in urban speaker recognition systems. *Computers and Electrical Engineering, 104 Part B*, 108446. DOI: 10.1016/j.compeleceng.2022.108446

Upadhyay, U., Kumar, A., Sharma, G., Saini, A. K., Arya, V., Gaurav, A., & Chui, K. T. (2024). Mitigating risks in the cloud-based metaverse access control strategies and techniques. *International Journal of Cloud Applications and Computing*, *14*(1), 1–30. DOI: 10.4018/IJCAC.334364

Villalonga, A., Negri, E., Biscardo, G., Castano, F., Haber, R. E., Fumagalli, L., & Macchi, M. (2021). A decision-making framework for dynamic scheduling of cyber-physical production systems based on digital twins. *Annual Reviews in Control*, *51*, 357–373. DOI: 10.1016/j.arcontrol.2021.04.008

Wang, B., Zhang, C., Sangaiah, A. K., Alenazi, M. J., & Al Qahtani, S. A., & K. S., S. K. (. (2024). Group consensus-driven energy consumption assessment using social network analysis and fuzzy information fusion. *International Journal on Semantic Web and Information Systems*, *20*(1), 1–32. DOI: 10.4018/IJSWIS.352043

Wang, D., Fu, Y., Liu, K., Chen, F., Wang, P., & Lu, C. T. (2023a). Automated urban planning for reimagining city configuration via adversarial learning: Quantification, generation, and evaluation. *ACM Transactions on Spatial Algorithms and Systems*, *9*(1), 1–24. DOI: 10.1145/3524302

Wang, D., Fu, Y., Wang, P., Huang, B., & Lu, C. T. (2020). Reimagining city configuration: Automated urban planning via adversarial learning. In *Proceedings of the 28th International Conference on Advances in Geographic Information Systems* (pp. 497–506). Association for Computing Machinery. DOI: 10.1145/3397536.3422268

Wang, D., Wu, L., Zhang, D., Zhou, J., Sun, L., & Fu, Y. (2023b). Human-instructed deep hierarchical generative learning for automated urban planning. *Proceedings of the AAAI Conference on Artificial Intelligence*, *37*(4), 4660–4667. DOI: 10.1609/aaai.v37i4.25589

Wang, J., Hadjikakou, M., Hewitt, R. J., & Bryan, B. A. (2022). Simulating large-scale urban land-use patterns and dynamics using the U-Net deep learning architecture. *Computers, Environment and Urban Systems*, *97*, 101855. DOI: 10.1016/j.compenvurbsys.2022.101855

Wang, L., Han, X., He, J., & Jung, T. (2022). Measuring residents' perceptions of city streets to inform better street planning through deep learning and space syntax. *ISPRS Journal of Photogrammetry and Remote Sensing*, *190*, 215–230. DOI: 10.1016/j.isprsjprs.2022.06.011

Wang, S., & Cao, J. (2021). AI and deep learning for urban computing. In Shi, W., Goodchild, M. F., Batty, M., Kwan, M.-P., & Zhang, A. (Eds.), *Urban informatics* (pp. 815–844)., DOI: 10.1007/978-981-15-8983-6_43

Wang, S., Liang, H., & Zhong, Y. (2023). *DeepMCLP: Solving the MCLP with deep reinforcement learning for urban spatial*. UC Santa Barbara: Center for Spatial Studies. DOI: 10.25436/E2KK5V

Ye, Q., Feng, Y., Candela, E., Escribano Macias, J., Stettler, M., & Angeloudis, P. (2021). Spatial-temporal flows-adaptive street layout control using reinforcement learning. *Sustainability (Basel)*, *14*(1), 107. DOI: 10.3390/su14010107

Yu, H., Wang, M., Lin, X., Guo, H., Liu, H., Zhao, Y., Wang, H., Li, C., & Jing, R. (2021). Prioritizing urban planning factors on community energy performance based on GIS-informed building energy modeling. *Energy and Building*, *249*, 111191. DOI: 10.1016/j.enbuild.2021.111191

Zhang, J., Zhang, X., Tan, X., & Yuan, X. (2022). Extraction of urban built-up area based on deep learning and multi-sources data fusion—The application of an emerging technology in urban planning. *Land (Basel)*, *11*(8), 1212. DOI: 10.3390/land11081212

Zheng, Y., Hao, Q., Wang, J., Gao, C., Chen, J., Jin, D., & Li, Y. (2024). A survey of machine learning for urban decision making: Applications in planning, transportation, and healthcare. *ACM Computing Surveys*, *57*(4), 99. Advance online publication. DOI: 10.1145/3695986

Zhou, L., Gaurav, A., Arya, V., Attar, R. W., Bansal, S., & Alhomoud, A. (2024). Enhancing phishing detection in semantic web systems using optimized deep learning models. *International Journal on Semantic Web and Information Systems*, *20*(1), 1–13. DOI: 10.4018/IJSWIS.361772

Jun Zhang is a professor and a doctoral supervisor in the College of Landscape Architecture at Northeast Forestry University. His research in healthy cities and urban design.

Liang Yimeng is an undergraduate student, majoring in urban and rural planning. Her research interests include town and country planning.